TEMPORAL TRENDS AND VARIABILITY IN THE SPATIAL DISTRIBUTION OF EUROPEAN TROPICAL TUNA PURSE-SEINE FISHING IN THE ATLANTIC AND INDIAN OCEANS

D.M. Kaplan[1][2]*, J.C. Báez[3], P.J. Pascual Alayon[4], T. Vidal[5]

SUMMARY

It is useful to complement more sophisticated stock status estimations based on stock assessment models with simpler approaches based on analyses of raw catch-effort data to maximize the probability of detecting overexploitation and hyperstability as early as possible. Here we develop a series of annual indices for the spatial distribution of catch over 1991-2019 by European purse seine vessels of the three major tropical tuna species as a function of ocean and fishing mode (floating object or free swimming fish schools). Time series of these indices are examined to identify temporal patterns with a focus on any long term trends that might be indicative of declining stock status or hyperstability. Spatial indices are also calculated for important bycatch species over 2011-2019 from observer data for French vessels. In general, results indicate a relative stability in the spatial distribution of catch over the last 30 years, though major perturbations, such as Somali piracy and major El Niño events, are identifiable. Nevertheless, recent decreasing trends in the presence of bigeye tuna and certain bycatch species merit further investigation.

RÉSUMÉ

Il est utile de compléter des estimations plus sophistiquées de l'état des stocks basées sur des modèles d'évaluation des stocks avec des approches plus simples basées sur des analyses de données brutes de capture-effort pour maximiser la probabilité de détecter la surexploitation et l'hyperstabilité le plus tôt possible. Nous développons ici une série d'indices annuels de la distribution spatiale des captures des trois principales espèces de thons tropicaux entre 1991 et 2019 par les senneurs européens en fonction de l'océan et du mode de pêche (sous objet flottant ou sur bancs libres). Les séries temporelles de ces indices sont examinées afin d'identifier toute tendance à long terme qui pourrait indiquer un déclin de l'état du stock ou une hyperstabilité. Des indices spatiaux sont également calculés pour les espèces accessoires importantes sur la période 2011-2019 à partir des données des observateurs des navires français. En général, les résultats indiquent une relative stabilité de la distribution spatiale des captures au cours des 30 dernières années, bien que des perturbations majeures, telles que la piraterie somalienne et les événements majeurs d'El Niño, soient identifiables. Néanmoins, les récentes tendances à la baisse de la présence de thon obèse et de certaines espèces de prises accessoires devraient faire l'objet d'une étude plus approfondie.

RESUMEN

Es útil complementar estimaciones más sofisticadas del estado de poblaciónes basadas en modelos de evaluación con métodos más simples basados en análisis de datos brutos de captura-esfuerzo para maximizar la probabilidad de detectar la sobreexplotación y la hiperestabilidad lo antes posible. Aquí desarrollamos una serie de índices anuales de la distribución espacial de las capturas de las tres principales especies de atunes tropicales entre 1991 y 2019 por los barcos cerqueros europeos en función del océano y el modo de pesca (objetos flotantes o bancos libres). Las series de tiempo de estos índices se examinan para identificar patrones temporales con un enfoque particular en cualquier tendencia a largo plazo que pueda ser indicativa de sobreexplotación o hiperestabilidad. También se calculan índices espaciales para las especies

---

1 Institut de Recherche pour le Développement (IRD), av. Jean Monnet, CS 30171, 34203 Sète cédex, France
2 MARBEC, Univ. Montpellier, CNRS, Ifremer, IRD, Sète, France
3 Centro Oceanográfico de Málaga, Instituto Español de Oceanografía, Puerto Pesquero, s/n Apdo., 29640, Fuengirola, Málaga, Spain
4 Instituto Español de Oceanografía, Dársena Pesquera PCL8, 38180 Santa Cruz de Tenerife, Spa
5 Pacific Community, CPS, BP D5, Noumea 98848, New Caledonia
* Corresponding author. Email: david.kaplan@ird.fr

de captura incidental más importantes durante 2011-2019 a partir de datos de observadores de barcos franceses. En general, los resultados indican una estabilidad relativa en la distribución espacial de las capturas durante los últimos 30 años, aunque se pueden identificar perturbaciones importantes, como la piratería somalí y los grandes eventos de El Niño. No obstante, las recientes tendencias decrecientes en la presencia de patudo y ciertas especies de captura incidental merecen una mayor investigación

1. Introduction

Catch per unit effort (CPUE) standardization (Maunder & Punt 2004) and model-based stock assessments (Methot & Wetzel 2013) are the gold standard for assessing the abundance and stock status of exploited species. However, these approaches are quite complex and at times it can be difficult to identify all pertinent covariants for estimating stock size while controlling for changes in fishing efficiency. If these approaches are not properly implemented, they can lead to hyperstability, wherein CPUE values remain constant despite stock decline (Walters 2003, Ward *et al.* 2013). Hyperstability can in turn lead to overly positive assessments of stock status, threatening fisheries sustainability and impairing management decision making.

Though there is currently no evidence that hyperstability is a problem in the tropical tuna purse-seine fisheries of the Atlantic and Indian Oceans, the subject of this study, it is important and consistent with the precautionary approach to fisheries management (de Bruyn *et al.* 2013) to use a multitude of complementary approaches to assessing fishery dynamics and stock status so as to maximize the probability of identifying problems as early as possible. In particular, though simpler spatial or temporal indices of fishing activity and catch cannot be used as direct indicators of stock abundance, they can highlight observed changes in fisheries and provide simple checks for more sophisticated approaches to stock status evaluation. For example, cases of hyperstability in the past have often been associated with increasing spatial concentration of fishing effort into the most productive areas without correction for this effect in CPUE standardization (Rose & Kulka 1999), thereby leading to the false impression that CPUE is remaining constant over all of space. Simple temporal characterizations of the spatial extent of fishing activity can be effective checks for this type of effort concentration, without using and independent of more sophisticated stock assessments.

Here we present analyses of the spatial distribution of catch and effort for the European tropical tuna purse-seine fisheries of the Atlantic and Indian Oceans. In addition to presenting basic exploratory statistics of the data, we develop a series of annual spatial indices for the catch of the three major species of tropical tunas, yellowfin tuna, (*Thunnus albacares*), bigeye tuna (*Thunnus obesus*) and skipjack tuna (*Katsuwonus pelamis*), as a function of ocean and fishing mode (i.e., floating object school or free-swimming fish school). Time series of these indices are examined to identify temporal trends and/or unique events with a particular eye towards any long-term trends that might be indicative of declining stock status and hyperstability in stock status estimates. Similar analyses are also carried out for the most important purse-seine bycatch species based on data from observers aboard French purse-seine vessels. Though the results are specific to the tropical tuna purse-seine fisheries examined, the spatial indices are generic and likely have wide applicability to other fisheries.

2 Materials & methods

This paper uses fine-scale (i.e., set level) logbook and observer catch-effort data from European tropical tuna fisheries of the Atlantic and Indian Oceans to assess temporal changes in the spatial distribution of the catch of major target and non-target species. First we present the data sources used for this study before presenting in detail the spatial statistics used to characterize these data.

2.1 Data

The data used for this study consist primarily of European tropical tuna purse-seine logbook observations of the catch of tropical tunas from 1991-2019. French data were provided by the French fleet via an agreement with ORTHONGEL, the French frozen tuna producers' organization, to the IRD-Observatory of Exploited Tropical Pelagic Ecosystems (Ob7) based in the MARBEC research laboratory. Similarly, Spanish data come from an

agreement between the principal Spanish frozen tuna producers organizations (ANABAC and OPAGAC) and IEO-CSIC (Spanish Institute of Oceangraphy). Logbook data include the name and unique identifier of the fishing vessel, the date and geographical coordinates of each fishing set, the type of fish school, and the catch in tonnes for each of the three main tropical tuna species. Fish schools type consist of schools associated with floating objects (i.e., FOB sets) and free swimming schools not associated with an object (i.e., FSC sets). Sets for which the school type was not noted were excluded from the data, as were null sets (i.e., sets for which the fishing vessel was unable to capture the associated fish school resulting in catch <1 tonne). The three major tropical tuna species with their abbreviations used in the text and figures are: yellowfin tuna (YFT), bigeye tuna (BET) and skipjack tuna (SKJ). Catch species composition data reported in logbooks were corrected based on port sampling using the T3 software (Pallarés & Petit 1998).

Logbook catch-effort data for the major tuna species were complemented with observer data for bycatch species from French purse-seine vessels. Observations were derived from three observation programs: the European Union Data Collection Framework (DCF, EU regulation 199/2008), the Moratoria program of the International Commission for the Conservation of Atlantic Tunas (ICCAT), and the OCUP program (Observateur Commun Unique et Permanent) of the French producer organization ORTHONGEL (Cauquil *et al.* 2015). As observer coverage of fishing activities was limited before ~2011, we examine data from the period 2011-2019. Within this period, observer coverage (in terms of number of positive sets for tuna with observer data) was low in both oceans during 2011-2013 (Fig. 1). From 2014 onward, observer coverage is more stable in both oceans, being close to 100% of the French fleet in the Atlantic Ocean (representing ~40-50% of the overall European logbook data used here) and approximately 40-50% of the French fleet in the Indian Ocean (representing ~20% of the European logbook data). As over 100 different species have been recorded in observer data, many of them being extremely rare, we focused analyses on just a few common or emblematic species and species groups: billfishes (multiple species from the *Istiophoridae* and *Xiphiidae* families), common dolphinfish (*Coryphaena hippurus*), rainbow runner (*Elagatis bipinnulata*), rays (individuals from the superorder *Batoidea*), silky shark (*Carcharhinus falciformis*) and wahoo (*Acanthocybium solandri*). Only landed or rejected-dead bycatch were included in our bycatch tabulations; live discards were not included.

2.2 Definition of positive sets for individual species

For some of the statistics presented in this paper (e.g., area of occupancy), it is necessary to decide if a given set is "positive" for a given species, i.e., whether the species can be considered to be present in the fish school. For the three major tropical tunas, a set will be considered "positive" for a species if the catch of that species exceeds 1 tonne or 5% of the overall set catch. This definition is necessary as corrections to the species composition of catch induced by T3 (Pallarés & Petit 1998) often assign small fractions of the catch to each species even if the true catch was actually zero for a species. 5% was chosen so that it represents 1 tonne for a 20 tonne set (roughly the mean set size), but small amounts for smaller sets.

For bycatch species, sets will be considered "positive" for a species if there is a non-zero observation of that species. This is appropriate for bycatch as bycatch levels are low with many absences, no corrections are applied to observer data for bycatch species, and observer data is generally quantified in terms of absolute numbers so that we have a true estimate of presence-absence.

2.3 Statistical analyses

Statistical analyses carried out can roughly be divided into three groups: (1) basic exploratory statistics, (2) spatial indices characterizing the area over which a species is observed (i.e., caught) by the fishery, and (3) indices of the spatial "inequality" or heterogeneity in catch. Basic exploratory statistics consisted of total catch per species, number of positive sets per species and the total area explored by the fishery, whereas the other two groups of statistics are developed below.

The basic statistical units of all analyses are $1° \times 1°$-year stratas. All data, including catches by species and number of positive sets by species, were first aggregated at this level before performing additional statistical analyses.

2.3.1 Characterizing the spatial extent of species observations

The spatial extent of species catch is assessed using two complementary statistics: area of occupancy (AO) and minimum area representing 90% of catch (D90). Whereas AO characterizes the total area over which a species is present, D90 characterizes the core area of catch for a given species. AO is calculated largely following *Vidal et*

al. (2020), except that we present both absolute AO (here referred to as aAO for clarity) values in units of area and relative AO (rAO), i.e., fractions of the total area explored by the fishery in a given year as presented in *Vidal et al.* (2020). aAO is the sum of the areas of the $1° \times 1°$ cells explored by the fishery in a given year weighted by the fraction of sets in each cell and year that are positive for a given species:

$$aAO_{y,\sigma} = \sum_{s \in S_y} \frac{x_{ys}^{\sigma}}{x_{ys}} A_s$$

where x_{ys} is the number of sets in cell s and year y, x_{ys}^{σ} is the number of sets in cell s and year y that are positive for species σ, A_s is the area of cell s, and S_y represents the set of cells explored in year y. For total catch, this index just reduces to the total area explored by the fishery in a given year, whereas for individual species area will be weighted by the rate of presence of the species.

Note that for simplicity, fish school type (i.e., FOB and FSC) and ocean indices are not shown in this and other equations in the paper as they apply implicitly to all variables.

The equation for rAO is the same as that for aAO, except that it is divided by the total area explored by the fishery in a given year:

$$rAO_{y,\sigma} = \frac{aAO_{y,\sigma}}{\sum_{s \in S_y} A_s}$$

As AO is sensitive to the number of outlier cells with small amounts of catch, D90 is also examined so as to assess the core area of species catch. D90 is calculated by first ordering the cells by the catch per unit area (CPUA):

$$CPUA_{ys,\sigma} = \frac{C_{ys}^{\sigma}}{A_s}$$

where C_{ys}^{σ} is the total catch of species σ in year y and cell s. This ordering differs from that used in Vidal *et al.* (2020), where cells were ordered by catch per set.

Once the $1° \times 1°$ cells have been ordered, we then sum the areas of the cells starting from the cells with the highest CPUA and going towards those with the lowest CPUA until the total associated catch represents at least 90% of the total catch for species σ in year y. The absolute area of these cells is referred to as the absolute D90 (aD90), whereas the same area divided by the total area explored by the fishery in a given year is referred to as the relative D90 (rD90).

For simplicity of interpretation, aAO and aD90 values are generally reported in units of the number of $1° \times 1°$ cells at the equator. As tropical tuna fishing largely occurs within ±20° latitude of the equator, the area of $1° \times 1°$ cells is nearly constant and reported aAO and aD90 values can be considered roughly equivalent to the raw number of cells. A $1° \times 1°$ cell at the equator has an area of 12,309 km2.

2.3.2 Indices of spatial heterogeneity

Spatial inequality or heterogeneity in catch value per species, ocean and fish school type were quantified using two related, but distinct, Gini statistics. The first is the standard Gini coefficient often used to quantify income inequality (Cowell 2000). This statistic is based on the Lorenz curve, which in our study context is a plot of the proportion of the total catch (of a given species, year and fish school type) as a function of the cumulative fraction of the all $1° \times 1°$ cells that are taken into account starting from those cells with the smallest catch. The Gini coefficient is defined as the area between the diagonal 45° line and the Lorenz curve. Though it is non-trivial to demonstrate, this area is mathematically equivalent to:

$$G_{y,\sigma} = \frac{\sum_{q \in S} \sum_{s \in S} |C_{yt}^{\sigma} - C_{ys}^{\sigma}|}{2 \sum_{q \in S} \sum_{s \in S} C_{ys}^{\sigma}}$$

where S is the total set of 1◦ × 1◦ cells explored by the fishery over the study time period. If catch is uniform among all cells (i.e., $G^\sigma ys \equiv G^\sigma ys$), then the Gini coefficient will be zero, whereas if catch is all concentrated in a single cell for a given year (but not other) then the Gini coefficient is one.

Given that tropical tuna purse seine fishing is primarily carried out close to the equator where 1◦ × 1◦ cells vary little in area (the maximum observed difference in cell area for our data is 11.8%), we will treat all cells as equivalent (i.e., as if they had the same area) when computing Gini coefficients.

The second inequality statistic used is the Gini Segregation Index (GSI) (Duncan & Duncan 1955). This index is also an area between the diagonal and a Lorenz curve, but this time the Lorenz curve is based on the difference between the proportion of the total catch in a 1◦ × 1◦ cell that occurred in a given year and the proportion of the total catch that occurred in all other years. The GSI essentially compares the spatial distribution of catch in a given year to that of all other years and is close to zero if those distributions are similar in a relative sense, i.e., the absolute magnitude of catch does not matter, but the catch in the given year must be high and low in the same places as that of other years. On the other hand, the GSI will be close to one if, for example, catch in one year occurs in very different places than that of other years, even if the total spatial extent of catch (e.g., number of 1◦ × 1◦ cells explored) is similar across years.

Mathematically, the GSI is calculated by first calculating the relative proportion of total catch in each year for each cell:

$$p^\sigma_{ys} = \frac{C^\sigma_{ys}}{\sum_z C^\sigma_{zs}}$$

(1)

These proportions and their complements are then cumulatively summed over cells:

$$X^\sigma_{ys} = \frac{\sum^s_{t \in S^\star_y} p^\sigma_{yt}}{\sum_{t \in S^\star_y} p^\sigma_{yt}}$$

$$Y^\sigma_{ys} = \frac{\sum^s_{t \in S^\star_y} \left(1 - p^\sigma_{yt}\right)}{\sum_{t \in S^\star_y} \left(1 - p^\sigma_{yt}\right)}$$

where S^*_y is the set of all cells explored by the fishery over the entire study time period ordered from the cell with the lowest value of p^σ to that with the highest value for target year y. Given these definitions, GSI is calculated as:

$$GSI^\sigma_y = \sum_{s \in S^\star_y} (X_s Y_{s-1} - X_{s-1} Y_s)$$

Note that unlike the Gini coefficient, GSI is not sensitive to differences in catch due to differences in 1◦ × 1◦ cell area. All cells are treated as one statistical unit of measurement, and due to the normalization across years for each cell in Equ. (1), cell area does not enter into the calculation.

2.4 Data processing & statistical tools

All raw data were stored in a PostgreSQL database (version 10.14-1) with the PostGIS extension for geospatial data (version 2.4.8). Though initial data aggregation and filtering was carried out in the database, further statistical analyses were carried out using R version 4.1.1 (2021-08-10) (R Core Team 2021). Gini coefficients were calculated using the Gini function in the R package ineq (Zeileis 2014), whereas Gini segregation indices were calculated using code developed following Duncan & Duncan (1955). Data visualization was carried out using the ggplot2 package (Wickham 2016).

Key R code for the functions used to calculate the indices discussed in this paper are provided in **Appendix A**.

3. Results

Results are first presented for the three major tuna species (YFT, SKJ and BET), before turning our attention to bycatch species.

3.1 Basic statistical analyses

Total catch varies in response to well-known changes in the tropical tuna purse-seine fisheries of the Indian and Atlantic Oceans (**Figure 2**). For example, the large increase in FSC catch in the Indian Ocean during the "golden years" (2003-2005) led to a shift in fishing vessels from the Atlantic Ocean to the Indian Ocean. This shift reversed itself after ~2007 due to the threat of piracy in the Indian Ocean. More recently, there has been an increase in FOB catch in both oceans, and in particular the Indian Ocean, both in absolute terms and at the expense of FSC catch. These changes are coincident with and likely driven by the advent of echosounder buoys (Wain *et al.* 2020) and the imposition of a YFT quota in the Indian Ocean since 2017.

There has been a long-term increase in the fraction of FOB catch that is SKJ in the Atlantic Ocean to the detriment of YFT and BET catch (**Figure 3**). In the Indian Ocean, no such long-term trend in FOB SKJ catch is visible, but there was a considerable decrease (increase) in the proportion of SKJ (YFT) catch from 2009-2013 that reversed itself after 2013. This reversal is coincident with the end of piracy in the Indian Ocean and the switch to echosounder buoys (Wain *et al.* 2020), though one would expect this latter change to impact both oceans. Also notable is the decline in FSC SKJ catch in both oceans, but particularly the Atlantic Ocean, after ~2005-2007. FSC SKJ catch has dramatically increased over 2017-2019 in the Indian Ocean at the expense of YFT catch, undoubtedly in response to the YFT quota. These changes are also visible in the number (**Figure 4**) and fraction (**Figure 5**) of FSC sets that are positive for SKJ and YFT. The fraction of positive sets also highlights the drop in the prevalence of (juvenile) BET in FOB sets in both oceans, but particularly the Indian Ocean, since ~2012-2013.

For the Atlantic Ocean, there has been a considerable increase in the catch of FSC BET in 2019. This agrees with anecdotal evidence from vessel captains who have noted a recent increase in the presence of BET in FSC sets.

Total catch per set has remained relatively stable over the study time period for all oceans and fishing modes (**Figure 6**). The most notable changes are the large increase in catch per FSC set in the Indian Ocean during the gold years period (2003-2005) due exclusively to an increase in YFT catch. FSC catch per set in the Indian Ocean has increased steadily since its minimum in 2007, with a noticeable uptick since 2017 (the year the YFT quota was put in place) due to a dramatic increase in SKJ catch in FSC sets. FOB catch per set values in the Indian Ocean were above average for the period 1999-2006 due to above average SKJ catch per set, before decreasing to a somewhat lower and stable value until 2016. Since 2017, FOB catch per set in the Indian Ocean has again been higher due to increased SKJ catch. Variability is lower in the Atlantic Ocean, though FOB catch per set was in 2019 close to its lowest value for the entire time series and FSC catch per set values were marginally above average for the period 2003-2008.

3.2 Indices of spatial distribution: AO and D90

aAO (**Figure 7**) and aD90 (**Figure 8**) for total catch show similar patterns, with values for FOB sets in the Indian Ocean being variable, but showing no clear trend, whereas the other series have clear jumps or trends. Areas for FSC catch show long term declines in both oceans since approximately the mid-2000's. There is a clear drop in FSC fished area for the Indian Ocean 2007-2011, from which Indian Ocean FSC fishing never recovers.

Perhaps the most noticeable temporal changes are the drop in Atlantic Ocean FOB fished area ~2005-2007 followed by a rapid rise in fished area ~2007-2010, after which FOB fished area more or less stabilizes at a new higher plateau than for the period preceding 2005. The drop 2005-2007 is seen in both FOB and FSC time series and is coincident with a period where numerous vessels moved from the Atlantic Ocean to the Indian Ocean in response to the "golden years" (2003-2005) in the Indian Ocean. The rise in FOB fished area 2007-2010 is coincident with the return of many vessels from the Indian Ocean to the Atlantic Ocean in response to Somali piracy, though other factors may also contribute: the increasing importance of FOB fishing over FSC fishing due to technological improvements and changes to the fishing fleet, changes in fishing agreements for access to coastal nation EEZs, and the effects of the 3-month, November-January FOB fishing moratorium in place 2009-2011 (Perez *et al.* submitted). The effect of the moratorium can be examined by comparing fished areas during the moratorium period to that of other months. Results indicate that the net increase in FOB fishing area occurred predominantly during the months outside the

moratorium period (**Figure 9**), the opposite of what one would expect for a moratorium effect. Similarly, a comparison of fishing zones 2000-2004 and 2010-2014 indicates that increases in fished area occurred predominantly in large offshore areas south and west/north-west of the core fishing zone, suggesting that changes in fishing agreements are not the driving factor, though they may play a role in certain specific areas, such as the absence of fishing off Senegal after 2010 (**Figure 10**).

rD90 for total catch, i.e., the ratio of aD90 to aAO, does not show a strong trend or variability for either ocean or school type (**Figure 11**). There is, however, a noticeable drop in rD90 for FOB fishing in the Atlantic during 2012-2015 and a slight increase in rD90 for FOB fishing in the Indian Ocean since 2015, neither of which has an obvious explanation. In general, D90 represents between 40% and 60% of the AO.

Areas of occupancy by species for the three major tropical tunas track each other much more closely for FOB catch than they do for FSC catch (**Figure 12**), highlighting the species specificity of FSC catch relative to FOB catch, though the relatively more important T3 corrections to FOB species composition cannot be ignored as a contributing factor. rAO values are also much closer to 1 for all three species for FOB catch than they are for FSC catch, confirming that FOB catches are generally mixed in terms of species compositions, whereas FSC sets are generally species-specific (with the exception of YFT that is generally present in FSC sets; **Figure 13**). The major trends include a decline in both oceans of BET presence in FOB catch since at least the early 2010's (and to a lesser degree YFT in the Atlantic), and the decline in SKJ prevalence in FSC catch since the early 2000's (though this decline has been eliminated since the imposition of the YFT quota in the Indian Ocean in 2017).

Absolute D90 (aD90) by species has similar patterns of variability to aAO, though the differences between the species for FSC catch are less marked (**Figure 14**). Relative D90 (rD90) values are approximately stable, though there does appear to be a slight concentration of YFT and BET FOB catch in the Atlantic Ocean since ~2013, as well as a long term concentration of SKJ and BET FSC catch in Atlantic Ocean since ~2007 (**Figure 15**).

4. Indices of spatial heterogeneity: Gini coefficient and GSI

Gini coefficients applied to annual catch data in general show similar trends for all three tuna species (**Figure 16).** Distinctions among species are more pronounced for FSC than FOB catch, and they are also more pronounced for the Atlantic Ocean than the Indian Ocean. Nevertheless, all three species track each other fairly closely and can be interpreted as an ensemble.

Values are higher (closer to one) for FSC than FOB indicating greater spatial heterogeneity/concentration for FSC. There is an overall, long term decreasing trend for FOB Gini coefficients, likely driven by the expansion of FOB fishing associated with technological advances in FOB tracking technology. On the other hand, FSC Gini coefficients increase over time indicating greater spatial concentration of catch as already observed in aAO and aD90 values (**Figures 12** & **14**). Gini coefficients for FOB fishing do appear to pick out major events in the fishery, e.g., the perturbations in the Indian Ocean in 1998 due to the El Niño event, the expanding use of dFADs since ~2015 and the effects of the YFT quota in the Indian Ocean since 2017.

Gini segregation index (GSI) results are more difficult to interpret, but generally show similar patterns and trends as do Gini coefficients (**Figure 17**). GSI does clearly pick up the unique distribution (leading to high GSI values) of FOB fishing in the Indian Ocean during the 1998 ENSO event, the 2003-2005 golden years period, the period impacted by Somali piracy (2007-2012) and the recent period impacted by the quota on YFT (2017-2019). The peak in the Atlantic for FOB fishing in 2007, followed by the dip around 2010 could be due to vessels moving back and forth between the two oceans in response to the golden years and Somali piracy. Surprisingly, the effect of Somali piracy is not particularly strong in the Indian Ocean and FSC GSI values only weakly reflect all these perturbations to the fisheries.

4.1 Bycatch data

As previously noted, observer coverage varied greatly over the period 2011-2014 (**Figure 1**). As such it makes little sense to look at absolute areas of occupancy for specific bycatch species as these primarily reflect changes in observer coverage itself for the early part of the time series. Therefore, we present only relative indices of spatial presence for bycatch species. Furthermore, the changing coverage over years made it impossible to standardize Gini indices of inequality (both the Gini coefficient and GSI) in a meaningful way across years, so these indices are not calculated.

Low observer coverage for 2011-2013 and ongoing rules permitting purse seine vessels to exclude observers in the Indian Ocean if there is a risk of Somali piracy can also lead to spatial bias in observations. In 2011-2013, coverage is sparse, but there do not appear to be strong spatial biases in core fishing areas, with the possible exceptions of the area off western Africa in the Atlantic Ocean and off Kenya and Tanzania in the Indian Ocean (left-hand panels in **Figure 18**). Over 2014-2019, coverage is much higher, but there is a noticeable bias in the Indian Ocean towards lower coverage in the vicinity of Somalia (right-hand panels in **Figure 18**). As such, care should be taken in interpreting trends and variability in results given these spatial and temporal biases.

4.1.1   *Basic statistical analyses*

As has been previously demonstrated (Amandé *et al*. 2010, Kaplan *et al*. 2014), bycatch rates for FOB sets are much higher than those for FSC sets (**Figures 19**). Observed FOB bycatch appears to increase over the study period for a number of species, such as rainbow runner, common dolphinfish and wahoo. Though this is undoubtedly driven by changes in observer coverage for the early part of the time series, at least some of the increase would appear to occur after 2013. There is a large peak in FSC billfish bycatch in the Atlantic Ocean for 2019, the origins of which are not immediately clear, but may be due to the stochastic nature of FSC bycatch.

The fraction of observed sets that are positive for each of the focus bycatch species, which should in principle be independent of changes in observer coverage provided that there is no spatial bias in coverage (which is not guaranteed), indicates that the prevalence of most species is roughly stable (**Figure 20**). Nevertheless, there are a few downward trends that merit future examination. For example, Indian Ocean FOB prevalence of common dolphinfish and wahoo appear to decline over the study period, as does Atlantic Ocean and Indian Ocean FSC prevalence of billfishes, rays and, to a lesser degree, silky sharks. However, much of these declines occur before 2013, putting into question their statistical significance. Furthermore, these declines could also be due to the implementation after ~2013 of best practices by most tuna RFMOs for handling and live release of bycatch species, particularly large, charismatic species, such as sharks and rays (Grande *et al*. 2020).

4.1.2   *Indices of area of presence*

Relative AO (rAO; **Figure 21**) and relative D90 (rD90; **Figure 22**) values for bycatch species reflect many of the same tendencies observed based on rates of presence in fishing sets (**Figure 20**). A number of species appear to have modest declines in area of presence in both FOB and FSC catch, but these decreases are largely, but not always entirely, concentrated in the early part of the time series when observer coverage was low.

5.   **Discussion**

This paper provides a simple set of spatio-temporal indices of catch and bycatch in European tropical tuna purse-seine fisheries of the Atlantic and Indian Oceans. Overall, results show no major signs of spatial concentration of fishing effort that would be indicative of hyperstability. Though there are long term trends and inter-annual variability, most of this can be attributed to either the long term shift of purse seine fishing from FSC to FOB sets or major perturbations to fishing effort, such as the 1998 El Niño, the golden years of the Indian Ocean (2003-2005), the impacts of Somali piracy (~2007-2012) and the imposition of a YFT quota for the Indian Ocean in 2017. Other potential sources of variability in the spatial distribution of fishing include the time-area FOB-fishing moratorium in the Atlantic Ocean and changes in the availability of fishing agreements giving access to the EEZs of certain countries (notably Senegal and Gabon in the Atlantic Ocean), though the analyses in this paper would suggest these are of lesser importance (**Figures 9** & **10**). Overall, these fishing strategy and effort distribution changes seem more plausible explanations of any observed trends than true changes in population size or distribution.

Nevertheless, there are a few trends that merit further investigation and continued vigilance. The modest decline in the presence of (juvenile) BET in FOB sets in both oceans does not have an immediate explanation. This could be related to technological changes in FOB fishing (e.g., the transition to echosounder buoys in ~2011-2012) or a response to the total allowable catch for BET in the Atlantic Ocean, which has been in place for a long time, but was notably reduced in 2016 (ICCAT 2015). Nevertheless, overfishing of juvenile BET on FOBs cannot be eliminated as an explanation. The analyses carried out in this paper should be repeated in the future to assure that this observed decline does not continue and if so, to better understand its origins.

Similarly, there are some indications of declines in certain bycatch species, such as common dolphinfish, wahoo and billfishes. Nevertheless, the short temporal extent of observer data and its low coverage in the initial years of the time series put into doubt the robustness of these observed trends. Though bootstrapping approaches could be used to assess uncertainty in statistical indices and standardize across years, we suspect that these indices would simply tell us what we already know - that bycatch rates are highly stochastic and subject to considerable uncertainties. Furthermore, as our data do not include live discards, observed decreasing trends, particularly for larger bycatch species, could be in part or entirely explained by best handling practices for live release of certain species (e.g., sharks, rays and billfishes) put into place after ~2013 (Grande *et al.* 2020). Given these uncertainties, it is in our view best to continue to follow these trends into the future so as to have longer and more reliable time series with which to assess changes in the prevalence of bycatch species. Comparing trends including versus excluding live discards could also be informative.

The statistical indices presented in this paper provide a standard set of tests that can be applied to data from a wide variety of fisheries to assess changes in the spatial distribution of catch of exploited species. Though not in and unto themselves useful as direct indicators of stock size or distribution, they can serve as red flags for changes that may be attributable to stock decline and hyperstability. As such, we believe that these simple statistical analyses should be a standard part of stock assessments both in tropical tuna fisheries and in many other fisheries worldwide.

References

Amandé M, Ariz J, Chassot E, Delgado de Molina A, Gaertner D, Murua H, Pianet R, Ruiz J, Chavance P (2010) Bycatch of the European purse seine tuna fishery in the Atlantic Ocean for the 2003-2007 period. Aquatic Living Resources 23:353–362. doi:10.1051/alr/2011003

Cauquil P, Rabearisoa N, Sabarros PS, Chavance P, Bach P (2015) ObServe: Database and operational software for longline and purse seine fishery data. IOTCWPEB11. Indian Ocean Tuna Commission 11th Working Party on Ecosystems & Bycatch (WEB11), Olhão, Portugal

Cowell FA (2000) Measurement of inequality. In: Atkinson AB, Bourguignon F (eds) Handbook of Income Distribution. Elsevier, p 87–166. doi:10.1016/S1574-0056(00)80005-6

de Bruyn P, Murua H, Aranda M (2013) The Precautionary approach to fisheries management: How this is taken into account by Tuna regional fisheries management organisations (RFMOs). Marine Policy 38:397–406. doi:10.1016/j.marpol.2012.06.019

Duncan OD, Duncan B (1955) A methodological analysis of segregation indexes. American Sociological Review 41:210–217. doi:10.2307/2088328

Grande M, Ruiz J, Murua H, Murua J, Goñi N, Arregi IKI, Zudaire I, Santiago J (2020) Progress on the Code of Good Practices on the Tropical Tuna Purse Seine Fishery in the Atlantic Ocean. Collect Vol Sci Pap ICCAT 76:193–234

ICCAT (2015) Recommendation by ICCAT on a Multi-Annual Conservation and Management Programme for Tropical Tunas. Rec. 15-01. International Commission for the Conservation of Atlantic Tunas

Kaplan DM, Chassot E, Amandé JM, Dueri S, Demarcq H, Dagorn L, Fonteneau A (2014) Spatial management of Indian Ocean tropical tuna fisheries: Potential and perspectives. ICES Journal of Marine Science 71:1728–1749. doi:10.1093/icesjms/fst233

Maunder MN, Punt AE (2004) Standardizing catch and effort data: A review of recent approaches.Fisheries Research 70:141–159. doi:10.1016/j.fishres.2004.08.002

Methot RD, Wetzel CR (2013) Stock synthesis: A biological and statistical framework for fish stock assessment and fishery management. Fisheries Research 142:86–99. doi:10.1016/j.fishres.2012.10.012

Pallarés P, Petit C (1998) Tropical tunas: New sampling and data processing strategy for estimating the composition of catches by species and sizes. ICCAT Collective Volume of Scientific Papers 48:230–246

Perez I, Guéry L, Authier M, Gaertner D (submitted) Assessing the efficiency of dFADs-fishing moratorium in the E stern Atlantic Ocean for conservation of juvenile tunas from AOTTP data.

R Core Team (2021) R: A language and environment for statistical computing. R Foundation for Statistical Computing, Vienna, Austria. Available from: https://www.R-project.org/

Rose GA, Kulka DW (1999) Hyperaggregation of fish and fisheries: How catch-per-unit-effort increased as the northern cod (Gadus morhua) declined. Canadian Journal of Fisheries and Aquatic Sciences 56:118–127. doi:10.1139/f99-207

Vidal T, Hamer P, Escalle L, Pilling GM (2020) Assessing trends in skipjack tuna abundance from purse seine catch and effort data in the WCPO. WCPFC-SC16-2020/SA-IP-09 Rev 1. Oceanic Fisheries Programme (OFP), The Pacific Community, Nouméa, New Caledonia

Wain G, Guéry L, Kaplan DM, Gaertner D (2020) Quantifying the increase in fishing efficiency due to the use of drifting FADs equipped with echosounders in tropical tuna purse seine fisheries. ICES Journal of Marine Science. doi:10.1093/icesjms/fsaa216

Walters C (2003) Folly and fantasy in the analysis of spatial catch rate data. Canadian Journal of Fisheries and Aquatic Sciences 60:1433–1436. doi:10.1139/f03-152

Ward HGM, Askey PJ, Post JR (2013) A mechanistic understanding of hyperstability in catch per unit effort and density-dependent catchability in a multistock recreational fishery. Canadian Journal of Fisheries and Aquatic Sciences 70:1542–1550. doi:10.1139/cjfas-2013-0264

Wickham H (2016) ggplot2: Elegant graphics for data analysis. Springer-Verlag New York. Available from: https://ggplot2.tidyverse.org

Zeileis A (2014) Ineq: Measuring inequality, concentration, and poverty. Available from: https://CRAN.R-project.org/package=ineq
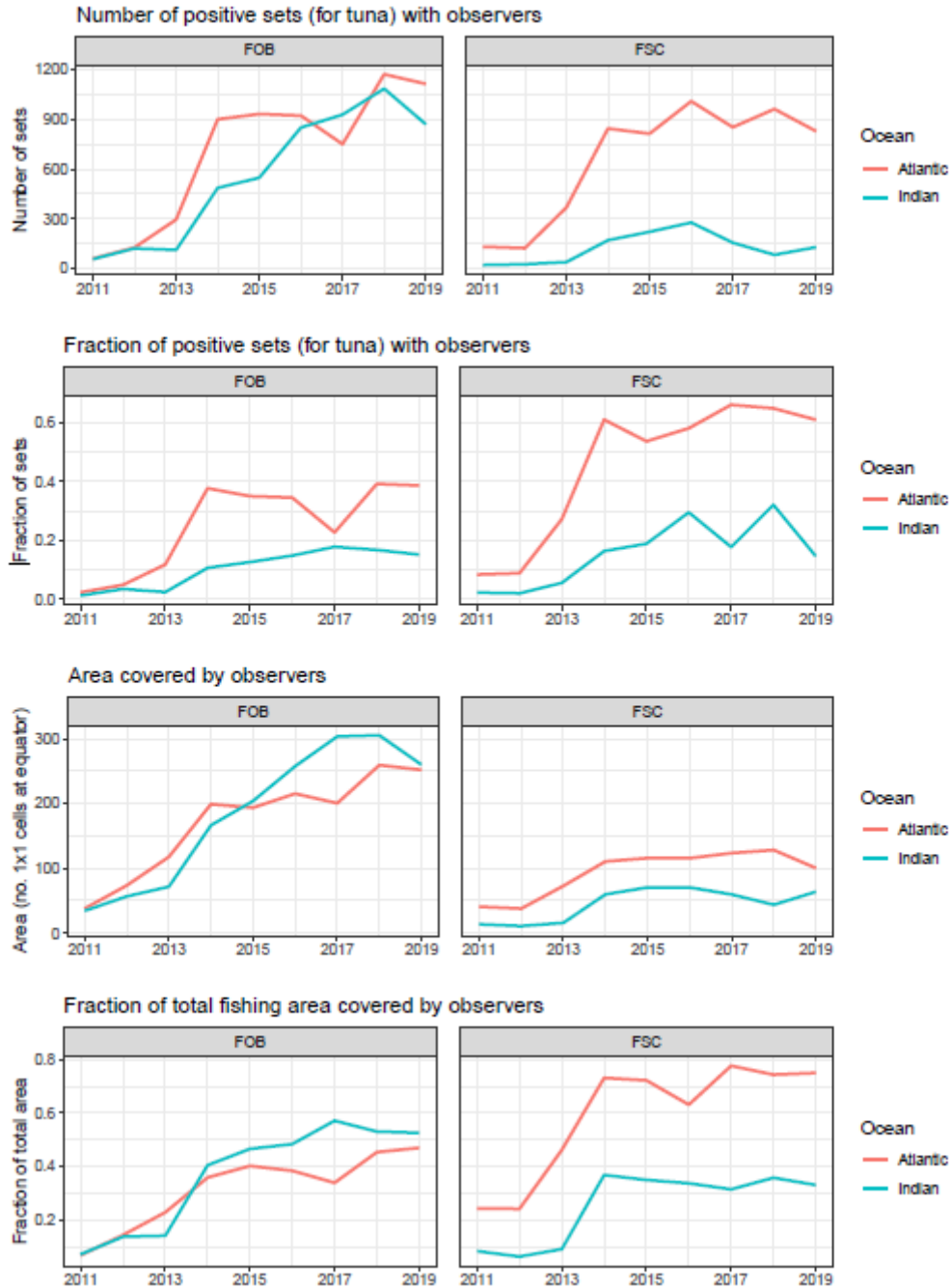
Figure 1. Coverage of observer data in terms of number of positive (for tuna) sets, fraction of all positive sets in the fishery, area and fraction of the total area explored by the fishery over time by ocean and fish school type. Fractions are calculated with respect to all European positive sets even though observer bycatch data is derived exclusively from French purse-seine vessels.

Total catch
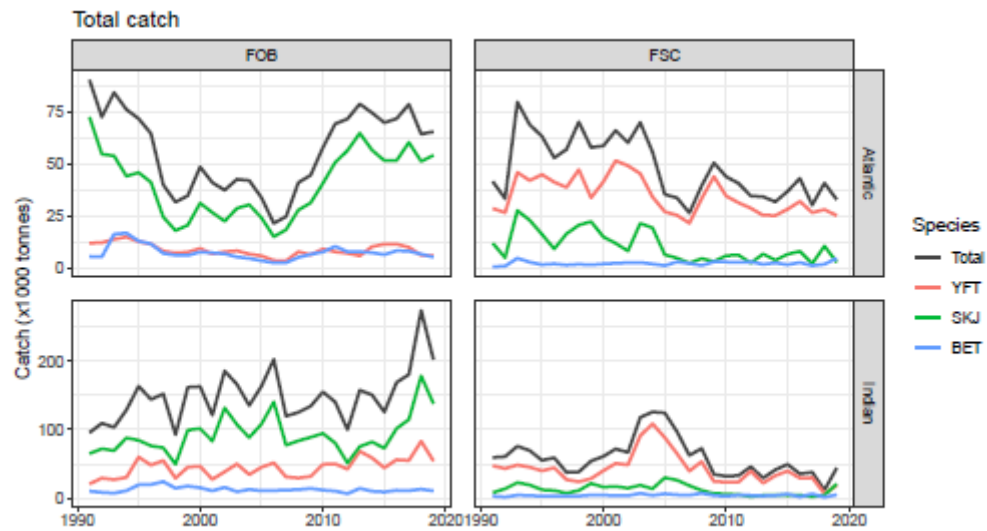
Figure 2. Catch per species as a function of year, ocean, and school type. Note that vertical scales differ between the bottom and top row of panels.

Fraction of catch for each species
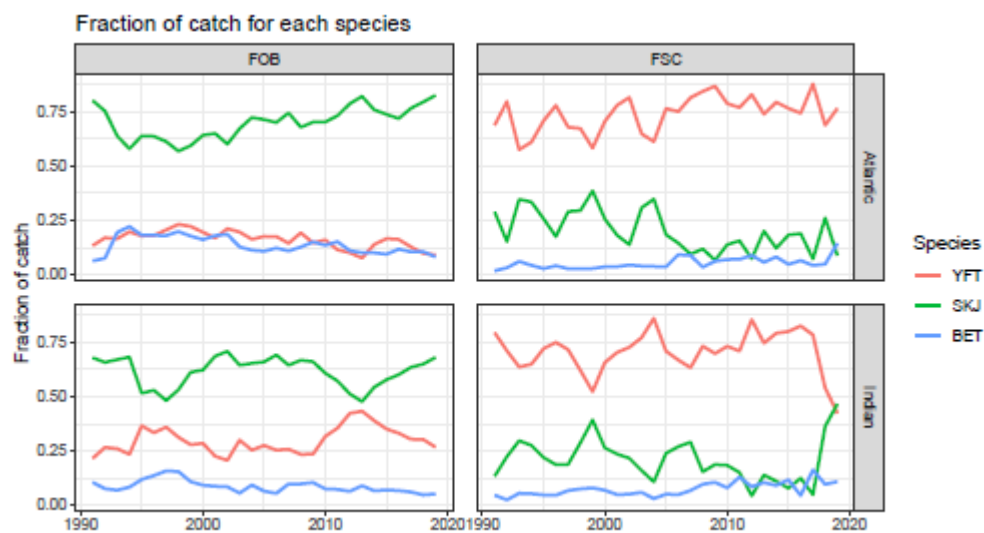
Figure 3. Fraction of catch by species as a function of year, ocean and school type.
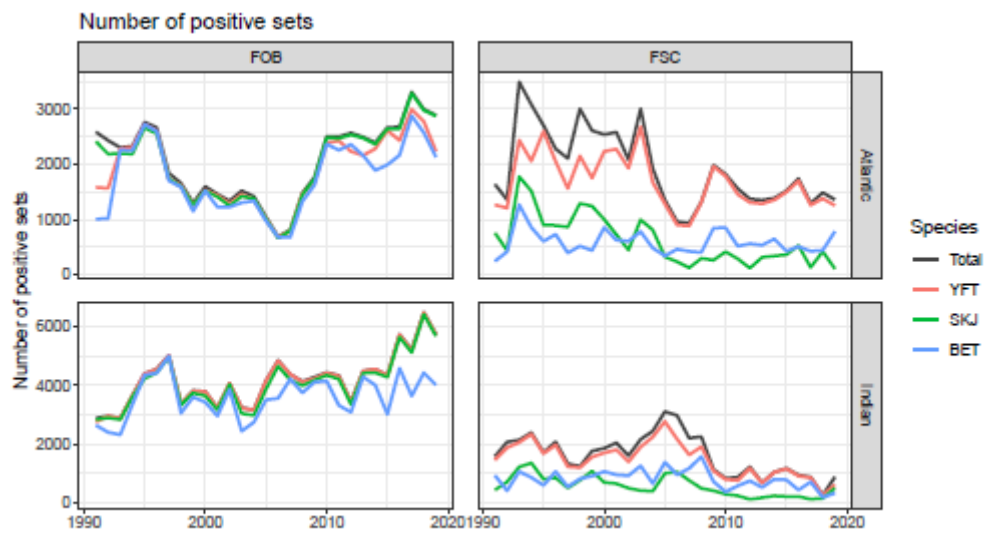
Figure 4. Number of "positive" sets as a function of year, ocean, school type and species. Note that vertical scales differ between the bottom and top row of panels
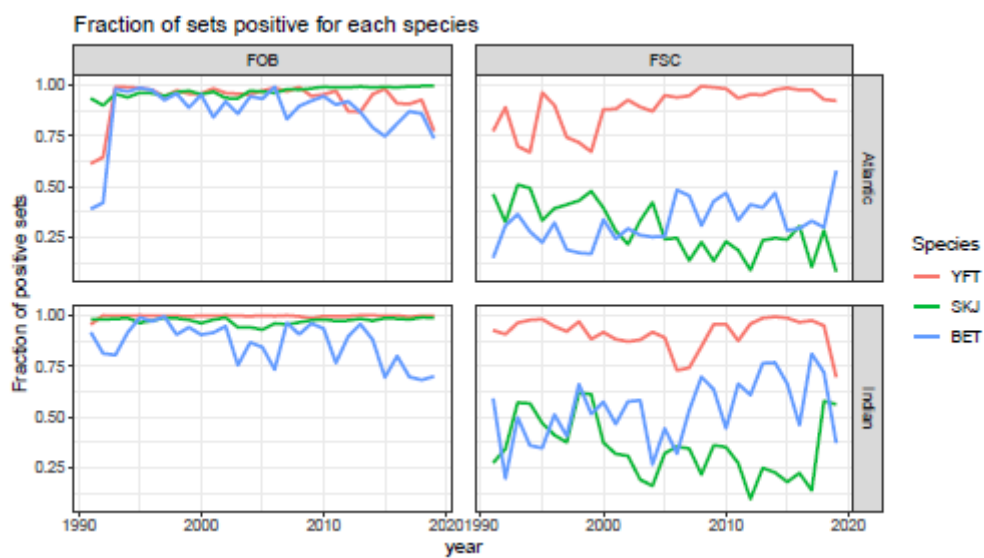
Figure 5. Fraction of sets in a given year that are positive for each species as a function of ocean and school type.
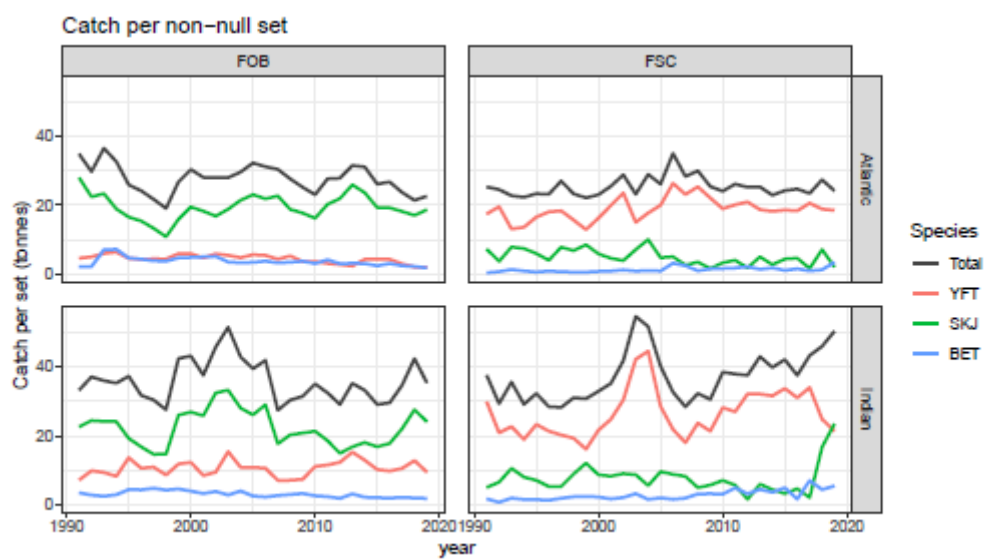
Figure 6. Catch of each species per set as a function of ocean and school type. Note that only non-null sets, i.e., those sets having a total catch >1 tonne, are included in the count of the number of sets.
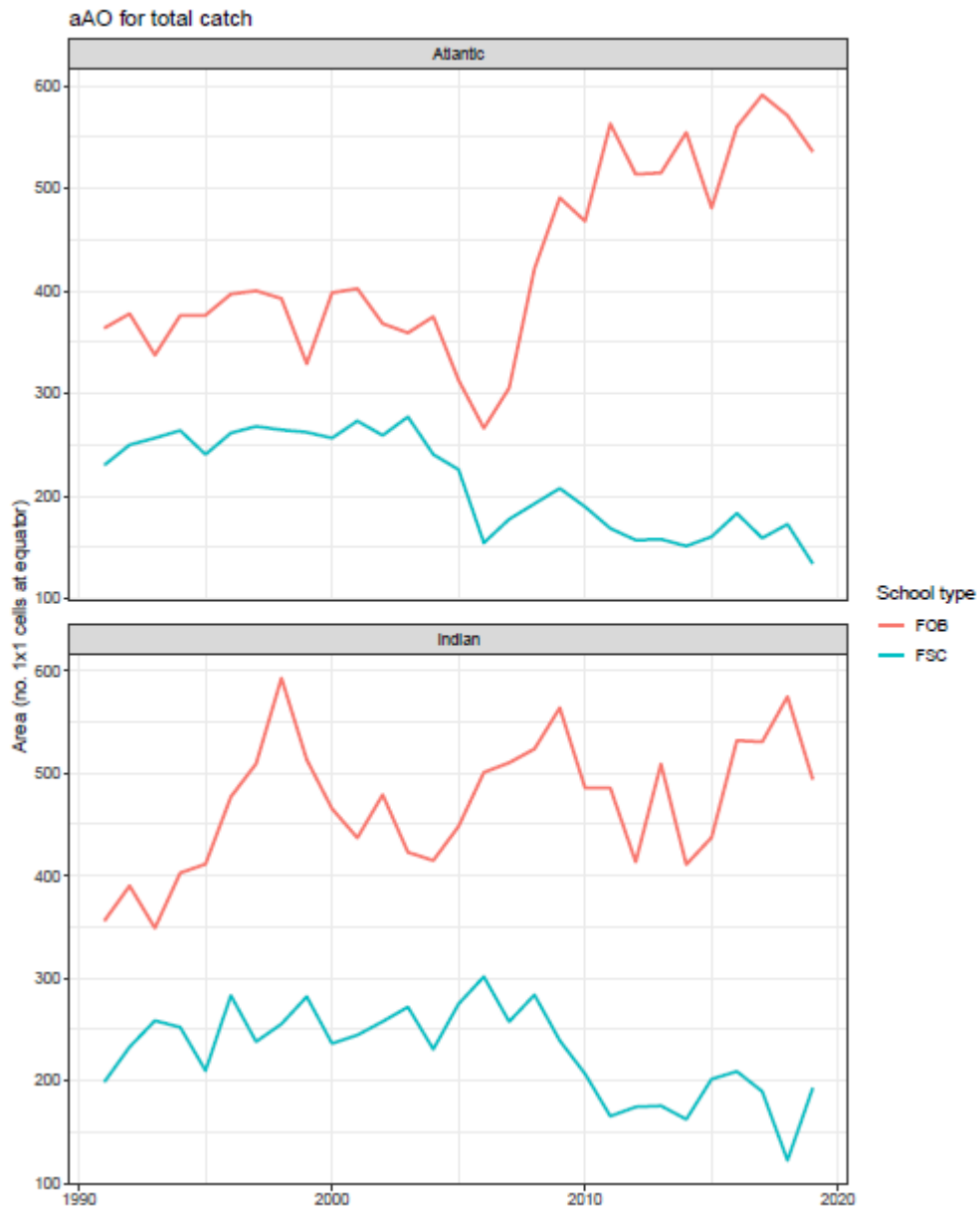
Figure 7. Total area over which the European fleet had at least one positive fishing set as a function of ocean, school type and year. Note that area is in units of 1x1 grid cells at the equator.
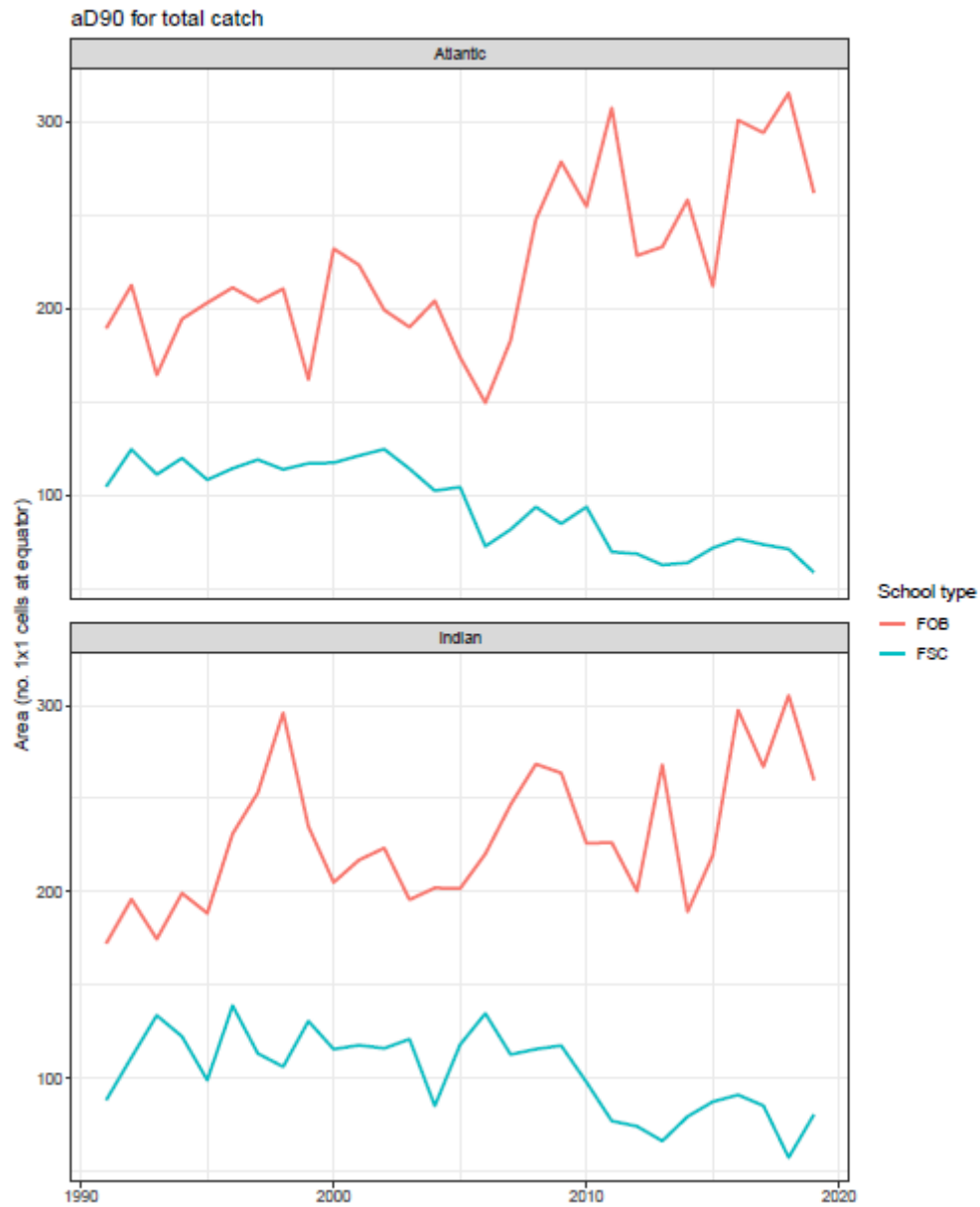
Figure 8. Minimum area representing at least 90% of the total catch as a function of ocean, school type and year. Note that area is in units of 1x1 grid cells at the equator.

aAO for total catch, Atlantic Ocean
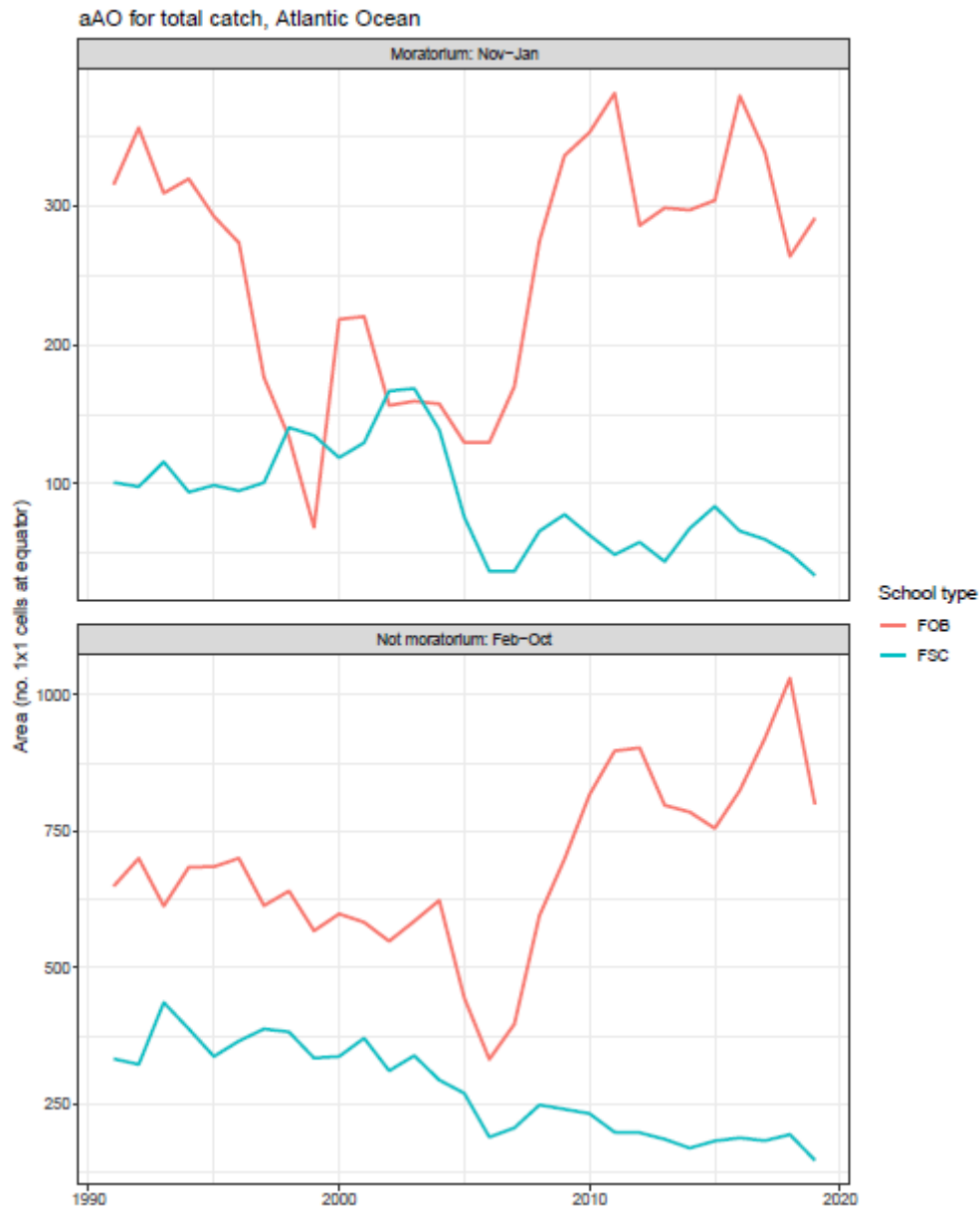
Figure 9. Total area over which the European fleet had at least one positive fishing set in the Atlantic Ocean as a function of period (moratorium or not), school type and year. Note that area is in units of 1x1 grid cells at the equator. The FOB-fishing moratorium from 2009-2011 corresponded to the months November-January

540
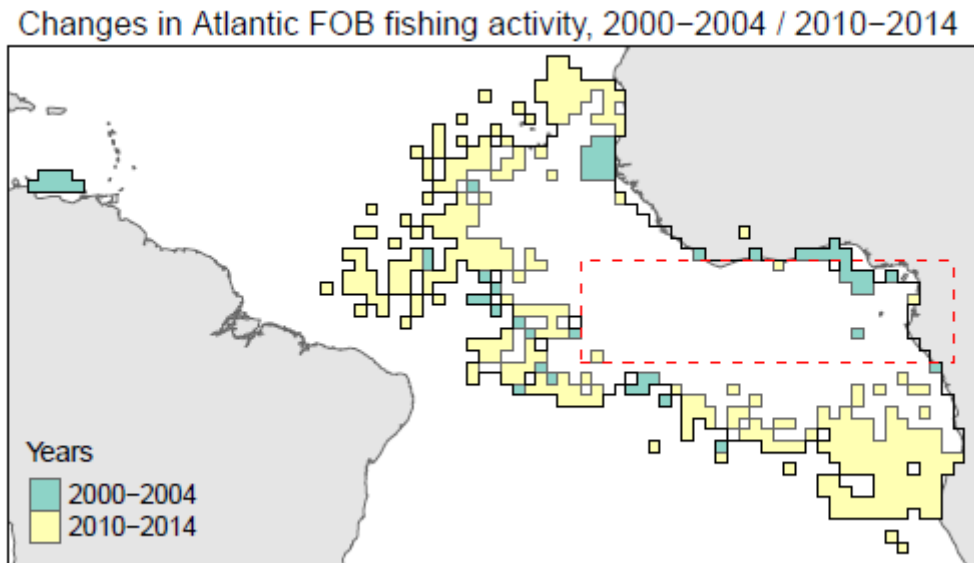
Figure 10. Differences in the distribution of European purse seine FOB fishing for the periods 2000-2004 and 2010-2014. Light green corresponds to areas fished at some point during 2000-2004, but not in 2010-2014. Light yellow corresponds to areas fishing during 2010-2014, but not 2000-2004. All other areas within the black polygon were fished in both years. The red dashed line indicates the November-January FOB-fishing moratorium zone in vigor 2009-2011.
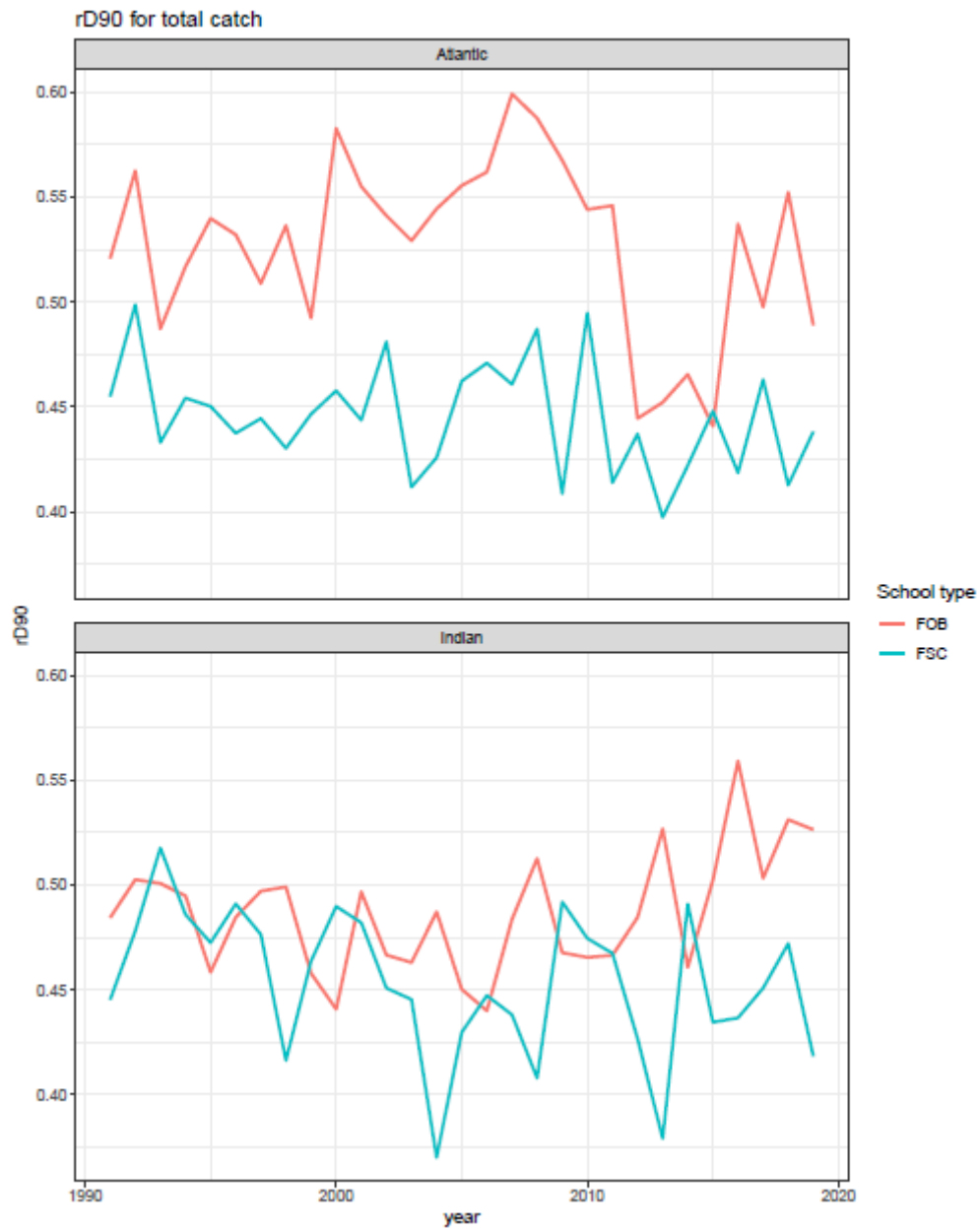
Figure 11. Ratio of aD90/aAO for total catch (i.e., rD90) as a function of ocean, school type and year.
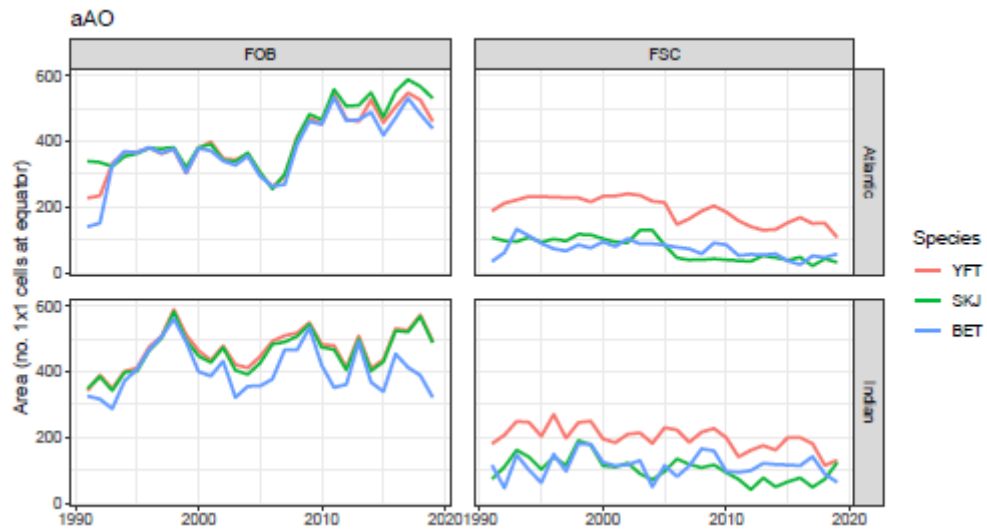
Figure 12. Absolute area of occupancy (aAO) as a function of year, species, ocean and school type.
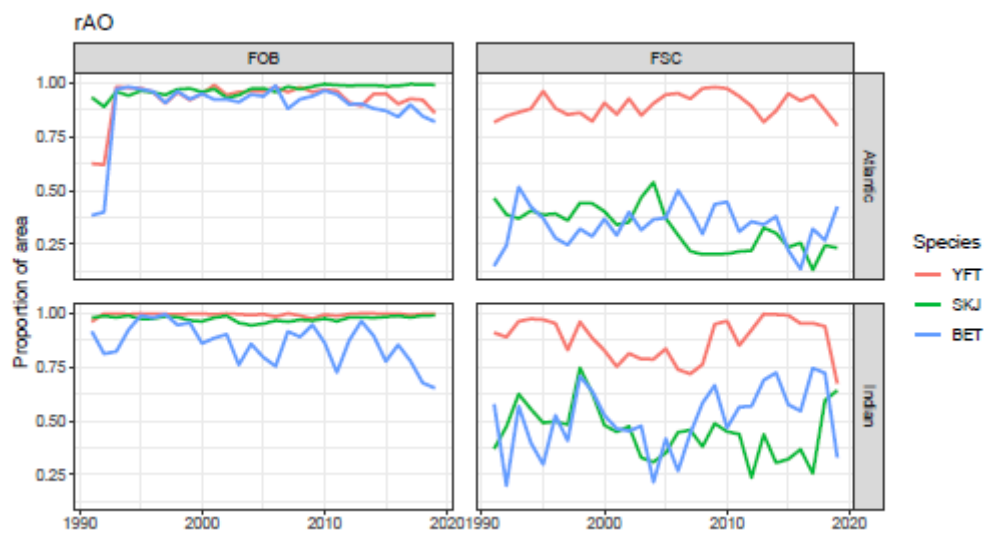
Figure 13. Relative area of occupancy (rAO) as a function of year, species, ocean and school type.

Figure 14. Minimum area representing 90% of catch (aD90) as a function of year, species, ocean and school type.
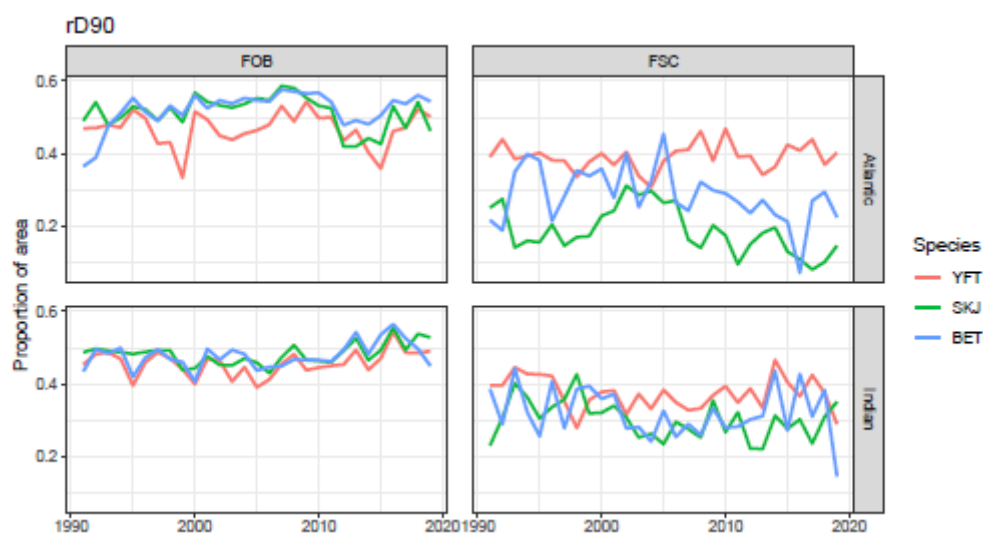
Figure 15. Minimum area representing 90% of catch relative to the total area explored by the fishery in a given year (rD90) as a function of year, species, ocean and school type.
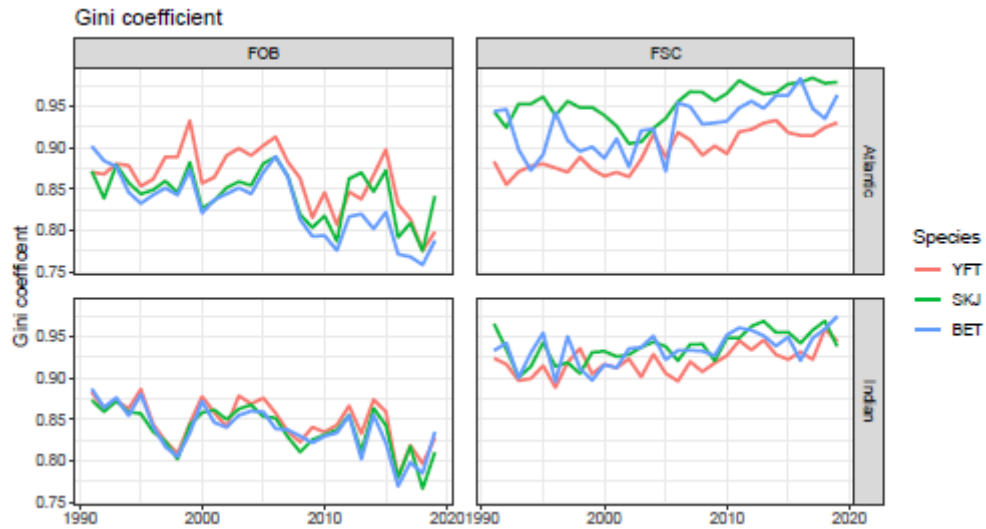
Figure 16. Standard Gini coefficient of catch per cell as a function of year, species, ocean and school type. Values close to 1 indicate fishing that is highly concentrated or otherwise very heterogeneous over space
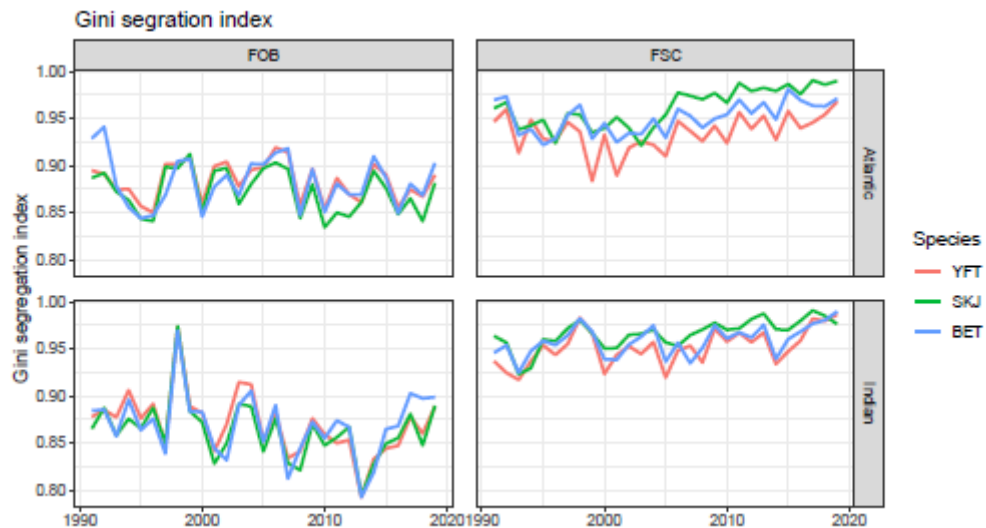
Figure 17. The Gini segregation index (GSI) of catch per cell as a function of year, species, ocean and school type. Values close to 1 indicate years that the spatial distribution of catch is highly   different from other years, either because of concentration or fishing being in unique spatial areas.
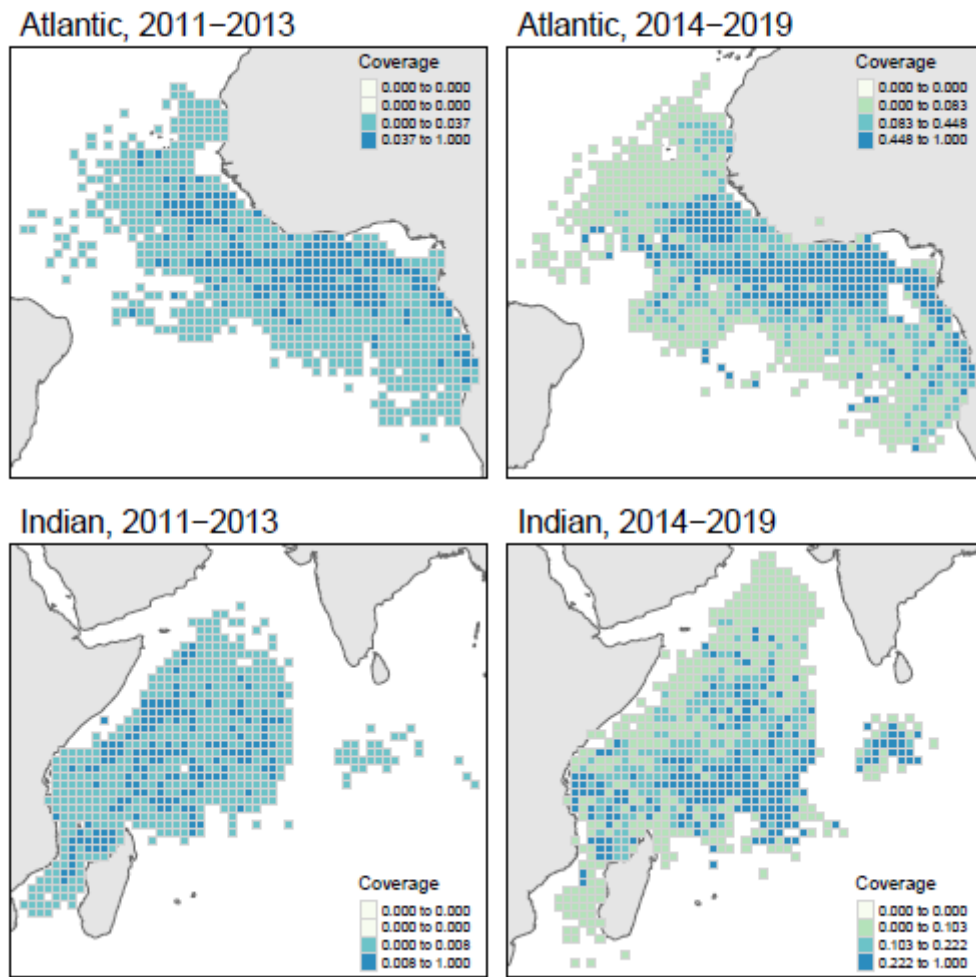
Figure 18. Spatial patterns of observer data coverage by ocean and period. Data is broken down into two periods: 2011-2013 and 2014-2019, corresponding to periods of low and high observer coverage, respectively. Note that coverage values are colored by quartile of the data so as to better highlight spatial biases.
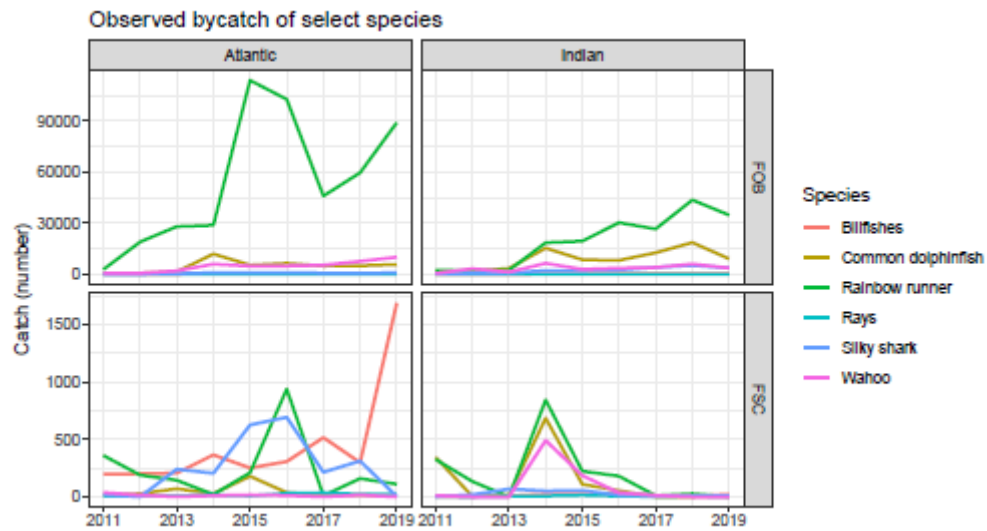
Figure 19. Total observer catch as a function of year, ocean, and species by school type.
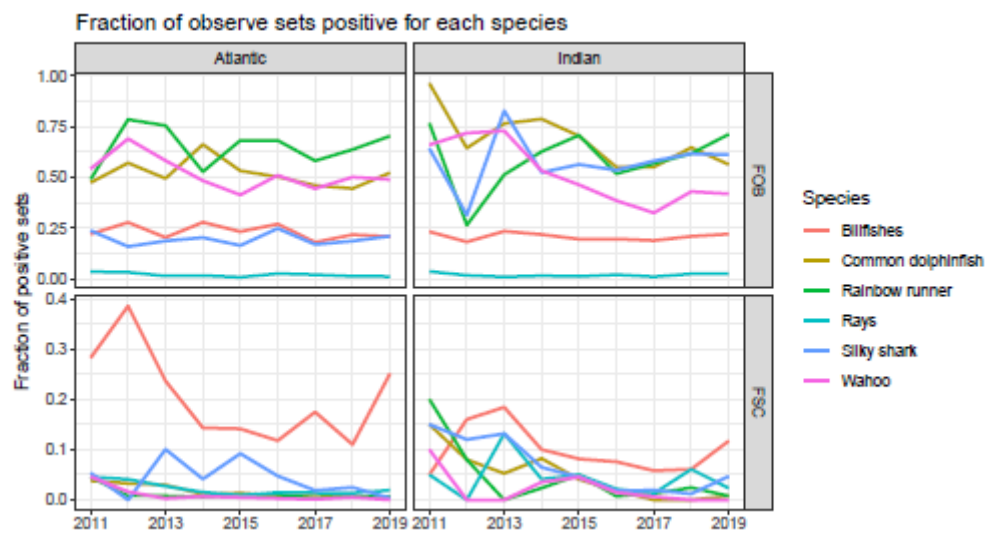

Figure 20. Fraction of sets with observer coverage in a given year that are positive for each bycatch species as a function of ocean and school type.
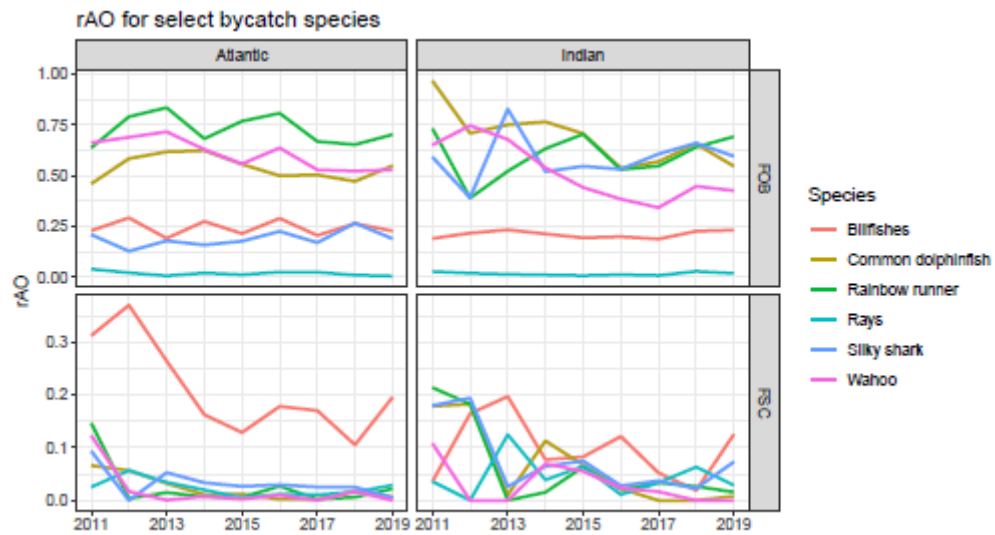
Figure 21. Relative area of occupancy (rAO) for bycatch species as a function of year, species, ocean and school type.
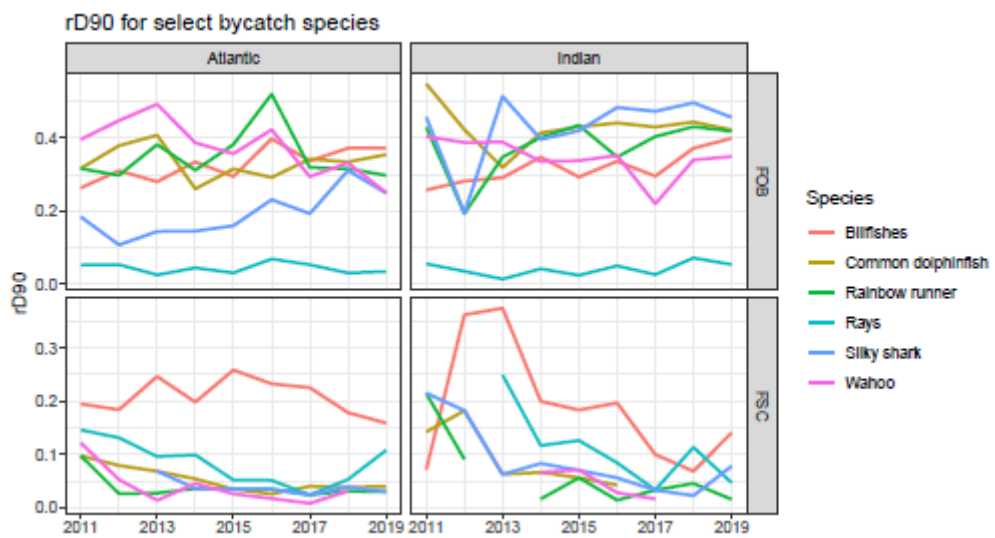

Figure 22. Minimum area representing 90% of catch relative to total observed area (rD90) as a function of year, species, ocean and school type.

548

Essential functions for calculating spatial indices

```r
# AO function - calculates both aAO and rAO
area_occupancy = function(pos_sets,num_sets,area) {
  aao = sum( pos_sets / num_sets * area)
  rao = aao / sum(area)

  return(c(absolute.ao=aao,relative.ao=rao))
}

# D90 function - calculates both aD90 and rD90
d90 = function(catch,area){
    I  =  order(-catch/area)
    catch  =  catch[I]
    area  =  area[I]

    cs = cumsum(catch) / sum(catch)

    ad90  =  cumsum(area)[min(which(cs>=0.9))]

    return(c(absolute.d90=ad90,relative.d90=ad90/sum(area)))
}

# Standard Gini coefficient. Should be the same as ineq::Gini
my.gini.coefficient = function(x) {
  v1 = sum(outer(x,x,function(y1,y2) abs(y1-y2)))
  v2 = 2 * length(x) * sum(x)

  return(v1/v2)
}

# GSI following formulas in Duncan 1955
my.gini.segregation.index = function(x) {
  #x <- OasisR::segdataclean(as.matrix(x))$x
  rs = rowSums(x)
  rs  =  ifelse(rs==0,1,rs)
  x = x / rs

  x  =  apply(x,2,sort)

  myf = function(X){
    s = sum(X)
    cumsum(X) / ifelse(s==0,NA,s)
  }

  y1  =  apply(x,2,myf)
  y2  =  apply(1-x,2,myf)

  n  =  nrow(y1)

  return(colSums(y1[-1,]*y2[-n,]-y1[-n,]*y2[-1,]))
}
```